

173 34
80123

Stability of Wavy Films in Gas-Liquid Two-Phase Flows at Normal and Microgravity Conditions

V. Balakotaiah

Department of Chemical Engineering, University of Houston, Houston, Texas 77204-4792

S. S. Jayawardena

NASA Lewis Research Center, Cleveland, OH 44135

Abstract:

For flow rates of technological interest, most gas-liquid flows in pipes are in the annular flow regime, in which, the liquid moves along the pipe wall in a thin, wavy film and the gas flows in the core region. The waves appearing on the liquid film have a profound influence on the transfer rates, and hence on the design of these systems. We have recently proposed and analyzed two boundary layer models that describe the characteristics of laminar wavy films at high Reynolds numbers (300-1200). Comparison of model predictions to 1-g experimental data showed good agreement. The goal of our present work is to understand through a combined program of experimental and modeling studies the characteristics of wavy films in annular two-phase gas-liquid flows under normal as well as microgravity conditions in the developed and entry regions.

1. Introduction

It is well known that for conditions of technological interest, there are three major types of flow regimes observed for gas-liquid flows in pipes at microgravity. At low gas flow rates, a 'bubbly flow' pattern, in which, small gas bubbles are uniformly distributed in the liquid, is obtained. Increasing the gas flow rate leads to 'slug flow'. This flow pattern is characterized by large bullet shaped gas bubbles separated by liquid slugs. Increasing the gas flow rate further leads to the 'annular flow' regime in which, the liquid moves along the pipe wall in a thin, wavy film and the gas flows in the core region. A large fraction of gas-liquid flows of practical interest under normal as well as microgravity conditions fall in the annular flow regime.

Experiments have shown that in the annular flow regime, the waves appearing on the liquid film have a profound influence on the transfer of heat, mass and momentum in these systems. Neglecting the wavy nature of the film can seriously underestimate the transfer rates. For example, the heat and mass transfer rates into the liquid may be enhanced by 100 to 300% in the presence of the waves as compared to the flat film case.

Our recent work focussed on the simplest form of the annular flow regime in which the liquid film falls under gravity through either a stagnant or an upward moving gas stream (causing interfacial shear). Fig.1 shows the experimentally measured film thickness profile for a freely falling film at a liquid flow rate of practical interest.

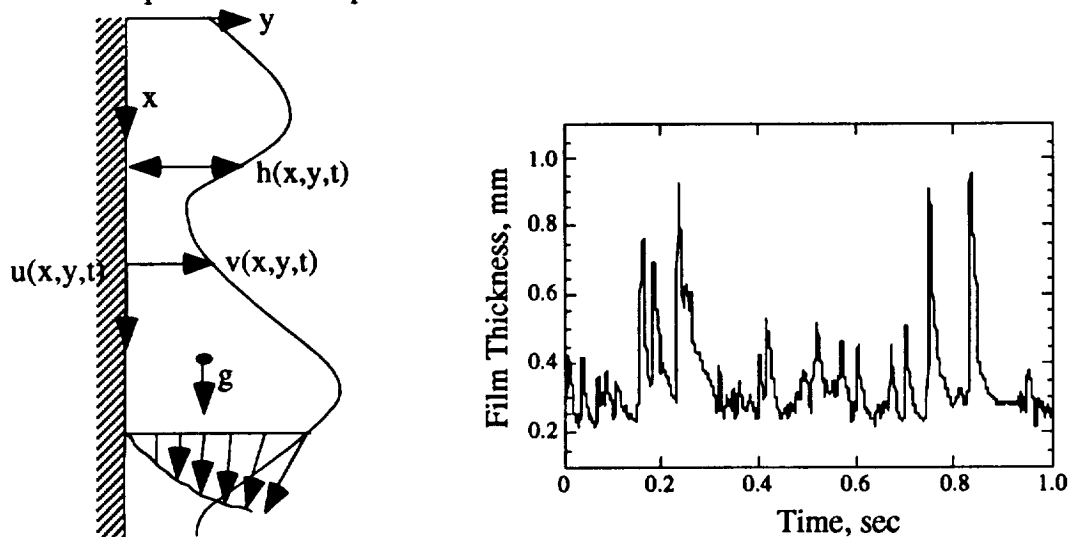


Fig.1: Schematic of a free falling film and experimentally measured film profile at $Re = 600$

The liquid film surface consists of a series of large waves accompanied by an array of wavelets of smaller amplitude and length which exist between these large waves. The large waves are steeper in the front and slope more gradually in the back with slopes not exceeding ten degrees. The amplitude of these large waves can be two to three times the mean film thickness and they carry a large fraction of the total mass flow. As shown above, the wave amplitude and spacing display a chaotic behavior similar to that observed in many lower dimensional deterministic models. It is speculated that the large waves contain stagnation points and recirculating regions which enhance the transport rates.

A major goal of our work is to develop predictive models for wavy films occurring in gas-liquid annular two-phase flows (as well as other applications) at normal and microgravity conditions and validate them with experimental data. We summarize here our recent results and outline the work in progress.

2. Boundary Layer Models for Wavy Films:

We have formulated two boundary layer models that are suitable for the description of laminar wavy films under normal gravity conditions [1]. The first model is the Kapitza's boundary layer model [2], which, for a two-dimensional film is given by the equations

$$\frac{Du}{Dt} = -\frac{1}{\rho} \frac{\partial p}{\partial x} + g + v \frac{\partial^2 u}{\partial y^2}; -\infty < x < \infty, 0 < y < h, t > 0 \quad (1)$$

$$\frac{\partial p}{\partial y} = 0 \quad (2)$$

$$\frac{\partial u}{\partial x} + \frac{\partial v}{\partial y} = 0 \quad (3)$$

$$u = v = 0 \quad @ \quad y = 0 \quad (4)$$

$$\frac{\partial u}{\partial y} = 0; \quad v = h_t + u h_x; \quad p - p_0 = -\sigma h_{xx} \quad @ \quad y = h \quad (5)$$

This model is based on the assumptions that the pressure in the film is independent of y , the tangential stress condition is the same as that for the Nusselt film and the normal stress condition includes only surface tension effect. This model is analyzed in some detail and it is shown that it is adequate for describing the statistics of large amplitude waves at high Reynolds numbers (in the range 300-1200). However, it is found that the model has one serious deficiency, i.e. it predicts negative wall shear stress at the front of a large wave on a free falling film. In addition, it cannot predict large waves with peak to substrate ratio exceeding 3 (observed in experiments).

We extended the Kapitza's model to include pressure variations across the film as well as higher order viscous terms in the x -momentum equation and tangential and normal stress boundary conditions. This *new second order boundary layer model* for a free falling film is described by the equations

$$\frac{\partial u}{\partial t} + u \frac{\partial u}{\partial x} + v \frac{\partial u}{\partial y} = -\frac{1}{\rho} \frac{\partial p}{\partial x} + g + v \left(\frac{\partial^2 u}{\partial y^2} + \frac{\partial^2 u}{\partial x^2} \right); -\infty < x < \infty, 0 < y < h, t > 0 \quad (6)$$

$$\frac{\partial p}{\partial y} = \rho h_{xx} u^2 \quad (7)$$

$$\frac{\partial u}{\partial x} + \frac{\partial v}{\partial y} = 0 \quad (8)$$

$$v = h_t + u h_x \quad \text{at } y = h(x,t) \quad (9)$$

$$\frac{\partial u}{\partial y} + \frac{\partial v}{\partial x} - h_x^2 \frac{\partial u}{\partial y} + 4 h_x \frac{\partial v}{\partial y} = 0 \quad \text{at } y = h(x,t) \quad (10)$$

$$p - p_0 - 2\mu \left(\frac{\partial v}{\partial y} - h_x \frac{\partial u}{\partial y} \right) + \sigma h_{xx} = 0 \quad \text{at } y = h(x,t) \quad (11)$$

$$u = v = 0 \quad \text{at } y = 0 \quad (12)$$

It should be noted that this model is much easier to solve than the full two-dimensional Navier-Stokes equations because of the highly simplified y-momentum balance equation. To assess the accuracy of the models, we compared the linear stability results for the three models, i.e. the boundary layer model (hereafter referred to as BL model), the second order boundary layer model (SBL model) and the complete set of two-dimensional Navier-Stokes equations.

We note that the Nusselt solution

$$p - p_0 = 0; v_0 = 0; h_0 = 1; u_0(y) = \frac{3}{2} (2y - y^2), 0 < y < 1$$

satisfies all three models (after transforming to dimensionless form using the Nusselt velocity u_N and film thickness h_N to scale the variables). Linearization of the model equations around this solution and simplification gives the Orr-Sommerfeld equation [3].

$$F'''' - 2\alpha^2 F'' + \alpha^4 F - \frac{i\alpha Re}{4} (u_0 - Ce)(F'' - \alpha^2 F) + \frac{i\alpha Re}{4} u_0'' F = 0 \quad (13)$$

$$F(0) = 0; F'(0) = 0; F(1) = Ce - \frac{3}{2}; F''(1) + \alpha^2 F(1) = 3$$

$$F'''(1) - 3\alpha^2 F'(1) - \frac{i\alpha^3 Re We}{4} + \frac{i\alpha Re}{4} F'(1)(Ce - \frac{3}{2}) = 0, \quad (13a)$$

where

$$\alpha = \pi \frac{h_N}{\lambda}, \quad Ce = Ce_r + iCe_i, \quad Ce = \frac{V_w}{u_N}, \quad (13b)$$

and V_w is the (dimensional) velocity of waves of infinitesimal amplitude. The function $F(y)$ represents the perturbation of the dimensionless streamfunction, We and Re are the Weber and Reynolds numbers defined by

$$We = \frac{\sigma}{\rho u_N^2 h_N} = 3^{1/3} 4^{5/3} Ka Re^{-5/3}; \quad Re = \frac{4\Gamma}{v} = \frac{4u_N h_N}{v},$$

$$u_N = \frac{gh_N^2}{3v}, \quad (\text{Nusselt average velocity}); \quad Ka = \frac{\sigma}{\rho g^{1/3} v^{4/3}}.$$

(The Kapitza number, Ka , has a value of 3371 for pure water at 25°C). The corresponding eigenvalue problem for the boundary layer model may be shown to be

$$F'''' - \frac{i\alpha Re}{4} (u_0 - Ce) F' + \frac{i\alpha Re}{4} u_0' F - \frac{i\alpha^3 Re We}{4} = 0 \quad (14a)$$

$$F(0) = 0; F'(0) = 0; F(1) = Ce - \frac{3}{2}; F''(1) = 3, \quad (14b)$$

while the second order boundary layer model gives

$$F'''' - \alpha^2 F'' - \frac{i\alpha Re}{4} [(u_0 - Ce)F' - u_0' F] - \frac{i\alpha^3 Re}{4} [1.2 + We - 0.45y^5 + 2.25y^4 - 3y^3] - 2\alpha^2 F'(1) = 0 \quad (15a)$$

$$F(0) = 0; F'(0) = 0; F(1) = Ce - \frac{3}{2}; F''(1) + \alpha^2 F(1) = 3. \quad (15b)$$

We compare in Fig. 2a the linear growth rate curves of the two boundary layer models with that of the Navier-Stokes equations (Orr-Sommerfeld analysis) for $Re = 600$ and $Ka = 3371$ (water). As can be expected intuitively, the curves nearly coincide for small wave numbers ($0 < \alpha < 0.4$) but the boundary layer model deviates significantly from other two for α values exceeding 0.5. Fig. 2b compares the critical wave numbers (on the neutral stability curves) for Reynolds numbers in the range zero to 1200 and $Ka = 3371$. From these comparisons, it may be concluded that the second order boundary layer model which includes pressure variations across the film and higher order viscous effects approximates the linear growth rate characteristics much better than the standard boundary layer model in the entire range of the wave numbers.

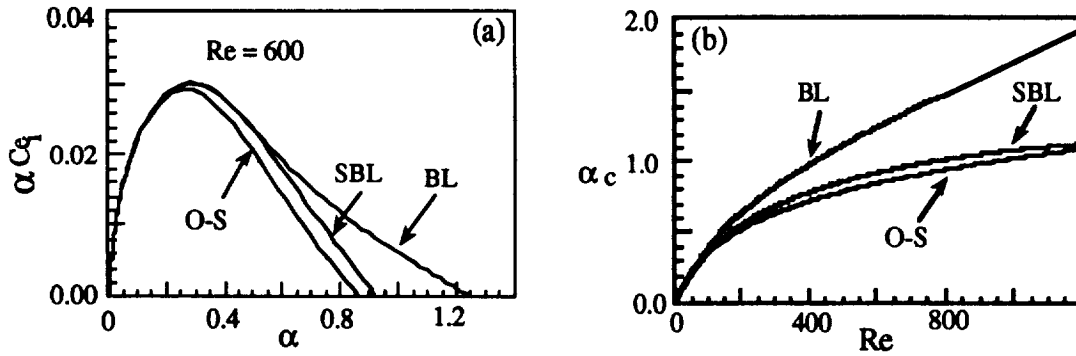


Fig. 2: Comparison of the linear growth rate and the neutral stability curves of the boundary layer models to the full Orr-Sommerfeld equation ($Ka = 3371$).

3. Numerical Solution Method and Comparison with Experimental Data:

In order to solve the boundary layer models, we developed a numerical scheme based on the boundary collocation method. We expand the streamfunction in the normal coordinate y ,

$$\Psi(x,y,t) = a_0(x,t) + a_1(x,t)y + \sum_{i=2}^n a_i(x,t)b_i(y) \quad (16)$$

where y is measured from the wall, x is the streamwise coordinate and t is time. The coefficients in the series, $a_i(x,t)$, are determined from both boundary and integral conditions as described elsewhere [3,4].

The polynomial expansion for $\Psi(x,y,t)$ is truncated at six terms to insure resolution of effects due to steep gradients, inertial forces, etc. The novel form of polynomial functions

$$b_i(y) = \left(y^i - \frac{(2i-3)y^{i+1}}{(2i-1)h} \right); \quad i = 2, 3, 4, 5 \quad (17)$$

is used. Here, $b_2(y)$ corresponds to parabolic flat film solution while b_3 , b_4 and b_5 account for deviation from parabolic profile and non-zero values for $\frac{\partial u}{\partial y}$ at the interface and the normal stress at the free surface. Determination of the coefficients $a_i(x,t)$ follows from substituting the assumed form of the streamfunction into various boundary and integral conditions. This procedure reduces (discretizes) the model equations into a set of coupled equations in x and t . These discretized evolution equations describe the film profile from wave inception to an asymptotic state, but their solution requires heavy computational efforts, because they are a set of highly nonlinear partial differential equations (of parabolic type) in t and x ($-\infty < x < \infty$). Results analogous to the linear stability are not available to describe the asymptotic form of the fully developed state. A systematic study of the fully developed steady film can be performed by transforming the equations to a traveling wave coordinate and reducing them to a finite dimensional set of ODEs whose behavior is parameterized by the wave celerity Ce . The computational procedure now requires only an initial condition (a perturbation upon a flat film) and yields the asymptotic behavior of the traveling waves.

A traveling coordinate system moving at a steady, nondimensional wave celerity Ce with respect to a stationary reference frame is defined by

$$z = x - Ce t \quad (18)$$

where z , x and t are physical coordinates normalized by h_N and h_N/u_N , respectively. We use this transformation and assume that motion with respect to the z coordinate is steady to reduce the partial differential equations into a set of six nonlinear ordinary differential equations.

We now present results of our simulations for the second order model and compare them with experimental data. We show in Fig.3 the computed film profiles at $Ce = 1.7457$ (below this

Ce value, no bounded solutions exist). Large waves with ripples in the front are interspersed between a random array of smaller waves. The streamlines for two large waves having peak to substrate ratio of 2.8 and 3.6, respectively are shown in Fig. 4. These streamlines clearly show the region of recirculation and how it increases with increasing peak to substrate ratio. This recirculation explains the experimentally observed heat and mass transfer enhancement in the presence of large waves. A comparison of the numerical results for the two models shows that both models predict the same qualitative behavior, but the second order model gives larger peak/substrate ratio and overcomes the main deficiency of the boundary layer model, i.e. negative wall shear stress at the front of large waves. We have calculated the flow fields in the film using the second order model and found that both $\frac{\partial p}{\partial y}$ and $\frac{\partial u}{\partial y}$ are not zero at the front of the large waves.

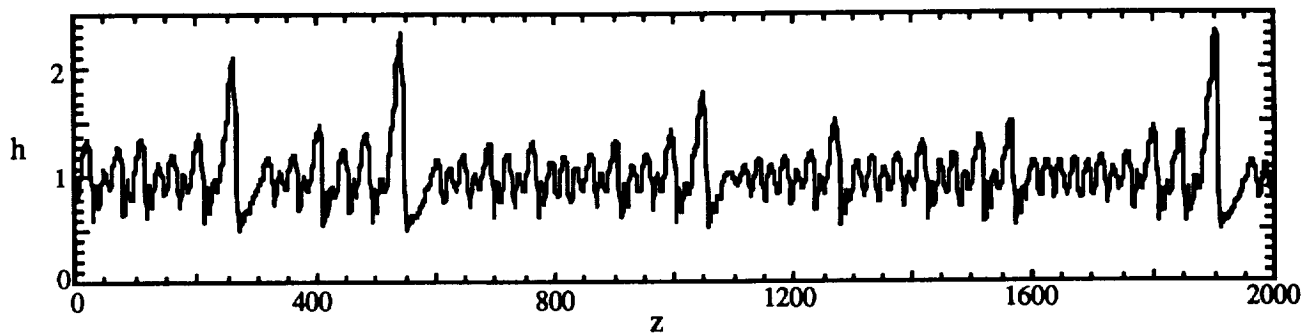


Fig. 3: Computed film profile for the second order boundary layer model and $Re = 600$, $Ce = 1.7357$ and $Ka = 3371$.

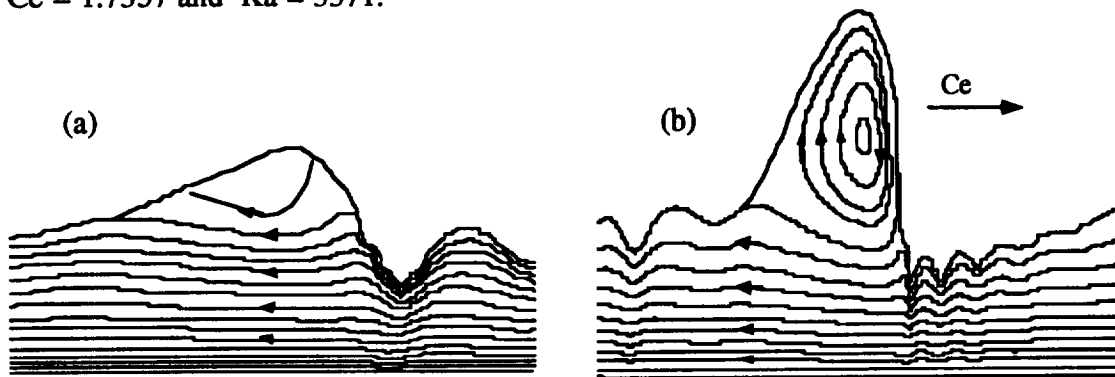


Fig.4: Computed streamlines under the large waves (in moving coordinate system) for peak thickness to substrate thickness ratio of 2.8 (a) and 3.6 (b).

We have compared the noise insensitive statistical properties of experimentally measured stationary wavy film profiles with the numerical results generated by integrating the model equations. The simulated waveforms are those obtained for the second order boundary layer model for a limiting wave celerity below which no bounded wave profiles exist. It was found that these chaotic waveforms have a structure similar to the naturally occurring (experimentally measured) traveling waves. Using the model equations, we have computed the wave celerity at inception (Hopf bifurcation), the celerity below which no bounded solutions exist, the rms film thickness, probability density function, power spectral density function and the mean and rms wave amplitudes using standard techniques. Fig. 5 shows good agreement between the computed and experimental values for celerity and rms film thickness. Similar agreement was also found for other statistical measures now shown here. The model equations show strong evidence that the wavy film is an example of a deterministic system displaying lower dimensional chaos.

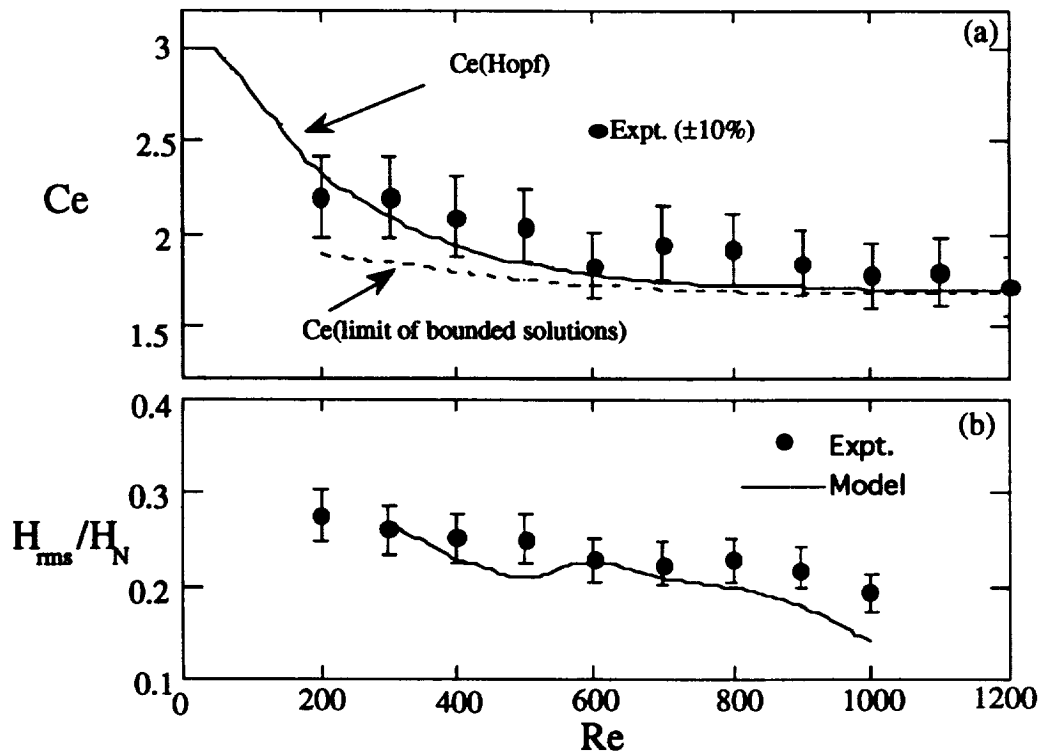


Fig. 5: Comparisons of computed wave statistics of chaotic film profiles ($Ka=3371$) with measured waveforms ($Ka=3350$). (a) Wave Celerity; (b) Wave rms film thickness.

4. Conclusions:

The second order boundary layer model presented here is the only model presently available in the literature to predict the behavior of wavy films at high Reynolds numbers. The initial results on the comparison of the model predictions to experimental data are very encouraging. However, the model needs further testing and refinement.

The major goals of our current work are (i) extension of the boundary layer models to predict the wavy film behavior in the presence of gas flow under normal and microgravity conditions (ii) experimental and modeling studies on two-phase developing flows to determine the evolution of the wavy structure on the gas-liquid interface and the length of the entry region of annular flows (iii) measurement and analysis of experimental data on pressure drop in fully developed two-phase annular flows in microgravity and (iv) to study the transition between annular and slug flow regimes, especially in microgravity.

5. References

- [1]. L.-Q. Yu, F. K. Wasden, A. E. Dukler and V. Balakotaiah, " Nonlinear Evolution of Waves on Falling Films at High Reynolds Numbers", *Physics of Fluids*, 7, 1866-1902 (1995).
- [2]. Kapitza, P. L. & Kapitza, S. P., "Wave flow in thin layers of a viscous fluid". *Zh. Exper. Teor Fiz.* 19,105(1949); also in *Collected Papers of P. L. Kapitza Vol. II*, Macmillan, NY (1964).
- [3]. Brauner, N., Moalem-Maron, D., "Modeling of Wavy flow in inclined thin films". *Chem. Eng. Sci.*, 38, 775 (1983).
- [4]. L.-Q. Yu, " Studies of Wavy Films in Vertical Gas-Liquid Annular Flows", Ph.D Thesis, University of Houston, Houston, Texas (1995).

Acknowledgements: This work described here was supported by the National Aeronautics and Space Administration under grants NAG9-854 and NAG3-1840.